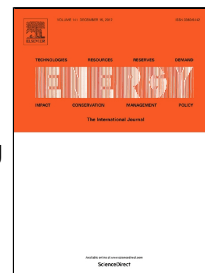


Accepted Manuscript

Experimental characterization of heat and mass transfer in a horizontal tube falling film absorber using aqueous (lithium, potassium, sodium) nitrate solution as a working pair



María E. Álvarez, Mahmoud Bourouis

PII: S0360-5442(18)30063-X
DOI: 10.1016/j.energy.2018.01.052
Reference: EGY 12164
To appear in: *Energy*
Received Date: 01 August 2017
Revised Date: 13 December 2017
Accepted Date: 09 January 2018

Please cite this article as: María E. Álvarez, Mahmoud Bourouis, Experimental characterization of heat and mass transfer in a horizontal tube falling film absorber using aqueous (lithium, potassium, sodium) nitrate solution as a working pair, *Energy* (2018), doi: 10.1016/j.energy.2018.01.052

This is a PDF file of an unedited manuscript that has been accepted for publication. As a service to our customers we are providing this early version of the manuscript. The manuscript will undergo copyediting, typesetting, and review of the resulting proof before it is published in its final form. Please note that during the production process errors may be discovered which could affect the content, and all legal disclaimers that apply to the journal pertain.

Experimental characterization of heat and mass transfer in a horizontal tube falling film absorber using aqueous (lithium, potassium, sodium) nitrate solution as a working pair

María E. Álvarez, Mahmoud Bourouis^{1*}

Department of Mechanical Engineering – Universitat Rovira i Virgili,
Av. Països Catalans No. 26, 43007 Tarragona, Spain.

*Corresponding author

Email: mahmoud.bourouis@urv.cat

Abstract

This paper deals with an experimental study which was carried out to investigate the absorption process with the aqueous solution of nitrates (Li, K, Na) in salt mass compositions of 53, 28 and 19%, respectively, used as a working fluid in a horizontal tube falling film absorber. This working fluid was proposed for use in the last stage of triple-effect absorption cooling cycles driven by high temperature heat sources (up to 260 °C). Taking into account these operating conditions, an experimental mini-absorber was designed and built. In a previous study, the optimal configuration of the solution distributor was determined based on flow visualisations to ensure a uniform distribution of the solution on the external surface of the tubes. A sensitivity study of the operating variables of the absorber was then carried out to evaluate a series of efficiency parameters for the absorber. At the operating conditions established in the experimental tests, the absorption rate ranged from 2.83 to 6.55 g.m⁻².s⁻¹, the heat transfer coefficient of the falling film varied between 631.9 and 1715.8 W.m⁻².°C⁻¹, while the mass transfer coefficient was between 2.1 x 10⁻⁵ and 6.0 x 10⁻⁵ m.s⁻¹.

Keywords: Aqueous nitrates solution, Alktrate, Horizontal tube falling film absorber, Triple-effect absorption cooling cycle, High-temperature heat sources.

Highlights

- The absorption process of aqueous solutions of nitrates is investigated.
- The working pair is confined to the last stage of a triple-effect absorption cycle.
- The absorber efficiency is similar to that of water/LiBr with additives.

ACCEPTED MANUSCRIPT

Nomenclature

A	Area	m^2
C_p	Specific heat	$\text{kJ.kg}^{-1} \text{ } ^\circ\text{C}^{-1}$
d	Tube diameter	m
h	Heat transfer coefficient on the solution side	$\text{W.m}^{-2} \text{ } ^\circ\text{C}^{-1}$
k_m	Mass transfer coefficient	m.s^{-1}
L	Tube length	m
m	Mass flow rate	kg.s^{-1}
Nu	Nusselt number	
P	Pressure	kPa
Pr	Prandlt number	
Q	Absorber thermal load	W
Re	Reynolds number	
T	Temperature	$^\circ\text{C}$
U	Overall heat transfer coefficient	$\text{W.m}^{-2} \text{ } ^\circ\text{C}^{-1}$
u	Velocity	m.s^{-1}
X	Solution concentration	Weight %

Greek letters

λ	Thermal conductivity	$\text{W.m}^{-1} \text{ } ^\circ\text{C}^{-1}$
-----------	----------------------	--

		1
μ	Dynamic viscosity	$\text{kg}\cdot\text{m}^{-1}\text{s}^{-1}$
ν	Kinetic viscosity	$\text{m}^2\cdot\text{s}^{-1}$
ΔT_{lm}	Logarithmic mean temperature difference	$^{\circ}\text{C}$
ΔT_{sub}	Subcooling	$^{\circ}\text{C}$
Γ	Solution mass flow rate per unit of wetted tube length (m/2L)	$\text{kg}\cdot\text{m}^{-1}\cdot\text{s}^{-1}$
ρ	Density	$\text{kg}\cdot\text{m}^{-3}$

Subscripts

abs	Absorber
c	Cooling water
Cu	Copper
Film	Falling film
i	Internal
In	Inlet
lm	Logarithmic mean temperature or concentration difference
o	External
out	outlet
s	Solution

v Vapour

eq Equilibrium

ACCEPTED MANUSCRIPT

1. Introduction

One of the most important applications of absorption refrigeration systems is the production of chilled water, using water/LiBr, for air conditioning technology. The objective of developing new absorption cooling cycles is to improve the coefficient of performance (COP) through advanced cycle configurations and to reduce the size of the components. Triple-effect absorption cycles represent a substantial improvement on performance compared to equivalent double-effect cycles. However, the operating conditions of triple-effect cycles are subject to challenges i.e. the working fluid mixtures and the materials must withstand high temperatures of above 180°C. Conventional working fluid water/LiBr cannot operate at these conditions without the use of corrosion inhibitors or resistant materials and also suffers problems of thermal instability. Therefore, current interest is in developing new thermally stable and non-corrosive absorbents for use in the triple-effect absorption cooling cycles that will take advantage of the thermal level of high temperature heat sources.

Erickson [1, 2] patented the use of aqueous solutions of nitrates and nitrites as working fluids in absorption heat pumps operating at high temperatures (260 °C). Subsequently, Davidson and Erickson [3] proposed a ternary solution composed of nitrates: LiNO_3 , KNO_3 , NaNO_3 with mass compositions in salts of 53%, 28% and 19%, respectively, as an absorbent for use in absorption refrigeration systems with high-temperature driving heat sources. Further, Erickson and Howe [4] called this absorbent by the name of "alkitrate". In their work, the authors showed the results of the first test conducted to measure the heat transfer coefficients of alkitrate carried out in an experimental facility. They used a simple vertical falling film absorber composed of a shell of 0.213 m in diameter and a tube (diameter 15 mm and height 1.52 m) where the solution was flowing down its outer surface. Although Erickson and Howe [4] did not conduct a systematic study on the heat and mass transfer characteristics of the aqueous solution of alkali nitrates; however, they conclude that this working fluid mixture was suitable for absorption cooling systems operating at high temperature heat sources (up to 260 °C).

Erickson et al. [5] investigated triple-effect absorption cooling cycles in which they proposed the use of water/alkitrate as an appropriate working fluid mixture because of its stability and non-corrosive nature. However, they warned of the risk of crystallization,

which may happen in cases of temperature drop or during a long period of inactivity of the equipment. Zhuo and Machielsen [6] simulated various configurations of a heat transformer using water/alkitrate as the working fluid. The authors reported that this mixture was of interest when operating at high temperatures (up to 260 °C) and COP values similar to those obtained with the conventional water/LiBr working fluid were achievable.

Álvarez et al. [7] numerically simulated the configuration of a triple-effect absorption cooling cycle denominated “cycle with a high temperature Alkitrate stage” (Figure 1). This configuration consisted of a double-effect cycle with parallel flow using water/LiBr as a working fluid and a single-effect cycle with alkali nitrate solution as the working fluid, coupled by means of heat exchange between the external streams. With this configuration there were no components exposed to corrosion and the alkali nitrate solution was confined to the high temperature stage because of the low range of solubility. The operating conditions of the high temperature Alkitrate cycle were established in order to obtain high values of the coefficient of performance (COP). Based on the simulation results, Álvarez et al. [7] built the Dühring diagram shown in figure 2 to be able to see the different streams of the cycle, the relative position of each component, and to check if the operating conditions of the cycle violated any design constraints. In figure 2, the triple-effect absorption cooling cycle with a high temperature stage that uses alkitrates as a working pair, operates at 4 pressure levels. The lines representing the crystallization temperatures for the aqueous solutions of LiBr and alkali nitrates were also included in the Dühring diagram, in order to observe the solubility areas of both working fluids. Indeed, a drawback of the aqueous solutions of alkali nitrates is the narrow range of solubility. However, at the operating conditions of the cycle investigated there is no evidence of a risk of crystallization.

Moreover, Álvarez [8] simulated the same configuration for the triple-effect absorption cooling cycle with lower mass concentrations of the solution at the high temperature stage. A high, but stable coefficient of performance (COP) of around 1,680 was obtained and without risk of crystallization. In this way, the appropriate operating conditions for the absorption process were established for the experimental study.

Recently, Asfand et al. [9] performed numerical simulations of a membrane-based absorber of the third stage of a triple-effect absorption cooling cycle using water/alkitrate

as a working fluid mixture. They reported that an absorption rate as high as 0.00523 kg/m².s was achievable with that kind of absorbers. In addition, they observed that the pressure drop percentage in the case of the water/alkitrate working fluid mixture was significantly lower because of the higher operating pressure.

Although the global market recognizes absorption refrigeration technology as an alternative to conventional vapour compression systems, absorption chillers are more expensive than compression systems, mainly because they require a greater number of components, which are also generally bigger in size. Thus, the high initial investment is the main drawback limiting the widespread application of absorption cooling systems. Generally, the absorber is the largest component in the absorption refrigeration unit. Thus, a way to improve the absorption process would be to reduce the size of the heat exchange area in order to obtain any significant reduction in the cost of the absorption machine.

In absorption chillers that use water as a refrigerant and a non-volatile component as an absorbent, the falling film absorber was generally the most commonly used design because it offered higher heat and mass transfer coefficients in the film region of the solution. In addition, drops in pressure are acceptable for the pressure conditions in these devices [10]. Several investigations reported in the open literature focused on the use of horizontal tube falling film absorbers and most of them used the water/LiBr pair as a working fluid mixture in their experiments.

In the present work, an experimental study was carried out to study the absorption process that takes place in a horizontal tube falling film absorber using aqueous solution of nitrates as a working fluid. At these thermal conditions, use of the conventional working fluid water/LiBr is not viable because of its thermal instability and corrosion. A sensitivity study was carried out varying the following operating parameters: mass flow rate and inlet temperature of the cooling water, mass flow rate of the solution, operating pressure of the absorber and concentration of the solution at the entrance of the absorber. As a result, the following performance parameters of the absorber were evaluated: the vapour absorption rate, the absorber thermal load, the degree of subcooling of the solution at the absorber outlet, the solution side heat transfer coefficient and the overall mass transfer coefficient.

2. Description of the experimental test facility

The test facility built to study the absorption process using the aqueous nitrate solution as a working fluid mixture, operated in continuous mode and recorded the operational data of the absorber and external circuits at different operating conditions. As shown in Figure 3, the experimental setup consisted of three main circuits: the solution circuit, the cooling water circuit and the vapour line. The main components of the experimental setup were the absorber, the steam generator, the auxiliary reservoirs and instrumentation. To avoid possible corrosion effects, 316L stainless steel was used as the building material. The pipe that connected most components had an outside diameter of 12.7 mm.

2.1. Solution circuit

The solution circuit consisted of a pump (SP), a heat exchanger cooled with the water network (HX1), a thermostatic bath (HB1) and two Coriolis flowmeters (C1 and C2). The solution circuit pump (SP) moved the solution from the bottom of the generator to the solution distributor (SD) at the top of the absorber. The solution pump worked at variable speeds and had a bladed turbine of EPDM (Ethylene Propylene Diene type M according to ASTM), an elastomeric polymer material well resistant to abrasion and wear, appropriate for viscous liquids and resistant to fluid temperatures of up to 160 °C. The heat exchanger (HX1) and the bath (HB1) were used to cool and control, respectively, the temperature of the solution entering the absorber. The coriolis flow meters (C1 and C2) were used to measure the mass flow rate, density and temperature of the solution with an uncertainty of 0.2% in the flow rate, 2 kg.m⁻³ in the density and 0.01 °C in the temperature measurement. The concentration of the solution of nitrates was implicitly obtained from the density and temperature measured by the Coriolis flow meters.

2.2. Cooling water circuit

The cooling water circuit was a closed circuit comprising a heat exchanger (HX2), a thermostatic bath (HB2) and a flow meter (FM). The cooling water introduced into the last tube of the absorber, circulated inside the tube bundle until it reached the first tube and then left the absorber. As the absorption process is exothermic, the cooling water

underwent an increase in temperature by dissipating the heat of absorption. To reduce the temperature of the cooling water a plate heat exchanger (HX2) was used. The heat exchanger HX2 used the network water circulating in a counter current flow direction with the inlet cooling water. The cooling water was cooled in the heat exchanger (HX2) to below the temperature required at the input of the absorber, so the temperature control was performed by heating in a thermostatic bath (HB2). The flow meter (FM) indicated the volumetric flow of cooling water to an accuracy of 0.8% of the full scale.

2.3. Vapour Pipe

A vapour pipe was used to move the water vapour produced in the generator to the absorber. The vapour pipe was flexible and made of stainless steel AISI 316 with an inside diameter of 50.8 mm. The pipe had a stainless-steel ball valve that allowed for the passage of water vapour to the absorber. The vapour pipe was connected to both the top of the generator and to the absorber by means of flanged joints.

2.4. Absorber

The absorber was the heart of the experimental setup built. It consisted of a cylindrical chamber of 600 mm in diameter and 590 mm in length, containing a copper tube bundle aligned horizontally and connected in series, a solution distributor at the inlet (SD) and a solution collection tray (CT) at the outlet of the absorber. Nitrate solution flowed through the outer surface of the tubes forming the falling film co-current with the vapour from the generator. The falling film formed on the outer surface of the tubes of the absorber was cooled with the cooling water flowing inside the tubes in the counter current direction to the solution. The internal view of the absorber is shown in Figure 4.

The tube bundle of the absorber was composed of 6 copper tubes with an outer diameter of 16 mm, a thickness of 1 mm and 400 mm in length. These tubes were in a fixed position with a separation of 30 mm between each of them. The tubes were connected in series by two 90° elbow joints at each step of the tube. In addition, a stainless-steel support kept the bundle of tubes fully aligned, and attached to the absorber chamber. The absorber had the facility for the assembly and disassembly of the tube bundle. This feature allows for the

bundle to be removed for cleaning or, if required, to make changes in its design. Moreover, a sliding bar was provided in the lower part of the chamber to maintain the arrangement of the tubes in a fixed position inside the absorber (Figure 4).

The aqueous nitrate solution coming from the generator entered the absorber chamber through a 25.4 mm stainless steel hose. The solution flow was divided into two streams by a "T" distribution system, which permitted feeding the distributor at both ends. The solution flowing over the surface of the tube bundle was collected in a collection tray, located in the bottom of the absorber, of the same length as the tubes and with a maximum capacity of 2.5 litres. The solution collection tray had a type of side flap with a 60° tilt angle that enhanced the size of the collection area and improved the collection and drainage of the solution.

Although the falling film absorber design is very common due to its practicality and performance, it has two main difficulties: poor wetting of the tubes and the need for better distribution of the solution entering the absorber. Poor wetting of the surface of the tubes and poor distribution of the liquid directly affect heat and mass transfer during the absorption process. To improve these inadequacies, firstly mechanical treatment was carried out on the outer surface of the six copper tubes forming the absorber (Figure 5). This consisted in the surface being slightly and proportionally roughened to enlarge the contact area, prevent preferential paths and improve the wetting of the tubes, as reported in previous studies [10, 11].

A systematic study on the performance of different configurations of the solution distributor at the absorber entrance was carried out by Álvarez [8] in order to obtain a design that would ensure a uniform distribution of the solution along the tubes of the absorber. Figure 4 shows the solution distributor integrated into the absorber tube bundle support. The liquid entered through each end of the inner tube of the distributor and, once it filled the total volume of the distributor, it overflowed through the holes located in the upper part of the outer tube. The configuration of the solution distribution system selected for the experimental device consisted of two concentric tubes, with solution inlets at each end (Figure 6). The outer tube of 12 mm external diameter had 39 small slots (7 mm long and 2 mm wide) which were laser perforated and oriented such that the liquid flowed upwards. The inner tube was longer than the outer tube, 8 mm in outer diameter, cut in half

longitudinally only in the inner section to the outer tube. The open section of the inner tube faced downwards. This configuration allowed for a uniform and stable solution flow to be obtained at the distributor outlet. The outer tube of the distributor underwent a light surface treatment, which avoided preferential paths being formed and improved the distribution of the solution, to create a uniform and homogeneous falling film.

Furthermore, the absorber was designed to allow for visual inspection of the falling film. Thus, it had two flanges of 340 mm outer diameter and 200 mm internal diameter, containing transparent borosilicate glass peepholes that allowed for inspection of the falling film flow and to verify that anomalies did not occur. Peepholes 257 mm in diameter and 15mm thick were located at each side of the absorber (one opposite the other).

2.5. Generator

The steam generator consisted of a cylindrical stainless-steel tank with a capacity of 30 litres and was responsible for supplying the water vapour entering the absorber. The vapour was generated by heating the solution contained in the tank by means of two electric resistance heaters (RG1 and RG2) of 2 kW each. The concentrated solution entering the absorber was also pumped from the generator. A solution pump (SP) provided the pressure needed to compensate the losses from height and head occurring before entering the absorber. Also, the diluted solution leaving the absorber returned to the generator.

2.6. Auxiliary equipment

The experimental setup had two auxiliary tanks, namely the solution preparation tank (ST) and the concentration control tank (WT). The ST reservoir was a cylindrical stainless-steel tank that was used for preparing the solution to be used as a working fluid in the absorber and for draining the equipment in the case of shutdown. The WT reservoir was also a cylindrical tank, which contained water for diluting or concentrating the solution entering the absorber. Its function was to store the water to be added to the solution circuit when it was necessary to reduce the salt concentration in the solution during experiments, and also

for the stored water to be drained from the solution circuit when a higher concentration in salt was required.

Due to the characteristics of absorption cooling cycles that use the solution of nitrates as a working fluid, the solution circuit, the generator and the absorber must all remain below atmospheric pressure. Therefore, it was essential to create a vacuum in the experimental device prior to commencing the experiment. A rotary vane vacuum pump was used to create a vacuum in the system at the desired pressure conditions. In order to guarantee the sealing of the experimental setup before carrying out the tests, the level of leakage was reduced to an accepted minimum as recommended by Beutler et al. [12]. At the end of the leak detection process after 2 days of pressure monitoring, the leak rate achieved always remained below 1×10^{-5} kPa.l.s⁻¹.

2.7. Instrumentation

Pt-100 4-wire platinum type thermal resistances (T) were installed to measure the temperature at various points in the system. To increase the precision of the temperature probes a calibration was carried out within the working temperature range (0-180 °C). The uncertainty in the temperature value associated with the calibrated PT-100 was ± 0.02 °C. The operating pressures of the absorber and the generator were measured with pressure transducers (TP) installed at the top of these components in the range of 0-5 bar absolute and were accurate to 0.04% full scale.

3. Experimental measurements

3.1. Measured parameters

To study the performance of a horizontal tube falling film absorber using nitrate solution as a working fluid, the following parameters were measured experimentally:

- Concentrated solution temperature at the inlet of the absorber, $T_{s,in}$. The solution was maintained at a subcooling temperature of 12 °C at the inlet of the absorber (Temperature T9 in figure 3).

- Temperature of the diluted solution at the absorber outlet, $T_{s, out}$ (Temperature T5 in figure 3).
- Absorber operating pressure, P_{abs} .
- Cooling water temperature at the absorber inlet, $T_{c, in}$ (Temperature T10 in figure 3).
- Cooling water temperature at the absorber outlet, $T_{c, out}$ (Temperature T12 in figure 3).
- Temperature and density of the solution at the inlet of the absorber ($T_{s, in}$ and $\rho_{s, in}$, respectively) measured by the coriolis C1, used to determine the concentration of the solution at the inlet of the absorber, $X_{s, in}$.
- Temperature and density of the solution at the outlet of the absorber ($T_{s, out}$ and $\rho_{s, out}$, respectively), measured by the coriolis C2, which served to determine the concentration of the solution at the absorber outlet, $X_{s, out}$.
- Mass flow rate of the concentrated solution at the inlet of the absorber, $m_{s, in}$.
- Volumetric flow rate of the cooling water in the absorber, m_c .

3.2. Test conditions

Experiments were carried out at the operating conditions defined by the simulation of a triple-effect absorption cooling cycle using aqueous nitrate solution as the working fluid [7, 8]. The operating conditions are listed in Table 1.

The solution was initially prepared in the preparation tank (ST). The amount of each of the salts was previously calculated and weighed and then introduced to maintain the desired mass proportions of 53:28:19 of LiNO_3 , KNO_3 and NaNO_3 salts, respectively. The compounds used were LiNO_3 (Fluka, 98%), KNO_3 (Fluka, 99%) and NaNO_3 (Panreac 98%) without further purification.

The effect on the performance of the absorber of the following variables was investigated; cooling water temperature and mass flow rate ($T_{c, in}$, m_c , respectively), solution mass flow rate (Γ), absorber operating pressure (P_{abs}) and solution inlet concentration ($X_{s, in}$). It is important to note that the rest of the operating conditions were kept constant in order to study the effect of each variable. However, some variables are closely related, therefore, criteria were established to make it possible to compare the different tests performed at the

same operating conditions. The performance of the absorber is dependent on the degree of subcooling of the solution at the inlet of the absorber [13]. If the solution enters the absorber with a higher degree of subcooling of the solution, the mass transfer process will start more quickly than in those cases where the solution inlet temperature is closer to equilibrium. If the solution enters the absorber at a temperature close to equilibrium, an amount of heat must be removed by the cooling water before the absorption process begins [14]. For this reason, the degree of subcooling of the solution at the inlet of the absorber was kept constant in all the experimental tests. The specific conditions used to study the effect of each variable are defined in the following sections.

3.3. Thermophysical properties of aqueous nitrate solutions

The thermophysical properties of the aqueous solutions of $\text{LiNO}_3+\text{KNO}_3+\text{NaNO}_3$, with a mass composition (53:28:19), were taken from a database [8], which contains experimental data and empirical correlations collected from the appropriate literature for the operating conditions established in the present study.

3.3.1 Vapour-liquid equilibrium of the solution

The polynomial equation developed by Álvarez et al. [15] was used for the vapour-liquid equilibrium. The authors adjusted the equation's parameters with the temperature and total mass fraction of salts at the liquid phase of the aqueous solutions of $\text{LiNO}_3+\text{KNO}_3+\text{NaNO}_3$ using their own experimental data. In addition, the authors built the Dühring diagram (PTX) for this mixture and included the crystallization line of the solution.

3.3.2 Density and dynamic viscosity

The mathematical expressions developed by Álvarez [8] in his doctoral thesis, which applied the approach of artificial neural networks (ANN), were used for the prediction of the density and dynamic viscosity of aqueous solutions of nitrates. The use of ANN to predict density and dynamic viscosity as a function of temperature and total mass fraction of salts was satisfactory, as evidenced by the low values of the root mean square error (rmse).

3.3.3 Other properties

Other properties of the working fluid such as specific heat, specific enthalpy and surface tension, which are important for the design and evaluation of absorption cooling cycles, were estimated using predictive methods obtained from the literature [8].

To estimate the specific heat, the authors used the model developed by Laliberté [16] for aqueous solutions constituted by several solutes. This model is valid for wide ranges of temperature and concentration. The correlation proposed by Ally [17] was used to calculate the specific enthalpy. This correlation is based on the data for the aqueous solution of $\text{LiNO}_3 + \text{KNO}_3 + \text{NaNO}_3$ with salt mass proportions of 53:28:19 obtained by Davidson and Erickson [18]. For the estimation of thermal conductivity and surface tension, expressions for multicomponent electrolyte solutions proposed by Aseyev [19] were used.

3.4. Performance parameters of the absorber

From the values of the variables measured, a series of parameters were calculated that served to analyse the operation of the absorber. These parameters are as follows:

The thermal load of the absorber was calculated from the flow rate of the cooling water circulating inside the absorber tubes and the temperature difference of the cooling water flowing through the tube bundle with the following equation:

$$Q_{\text{abs}} = m_c C_{p_c} (T_{c,\text{out}} - T_{c,\text{in}}) \quad (1)$$

The logarithmic mean temperature difference in the absorber (ΔT_{lm}) was calculated using the solution temperatures at the inlet and outlet of the absorber and the inlet and outlet temperatures of the cooling water [10, 20, 21]

$$\Delta T_{\text{lm}} = \frac{(T_{s,\text{in}} - T_{c,\text{out}}) - (T_{s,\text{out}} - T_{c,\text{in}})}{\ln \left(\frac{(T_{s,\text{in}} - T_{c,\text{out}})}{(T_{s,\text{out}} - T_{c,\text{in}})} \right)} \quad (2)$$

The thermal load of the absorber and the logarithmic temperature difference were used to calculate the overall heat transfer coefficient:

$$U = \frac{Q_{\text{abs}}}{A_o \Delta T_{\text{lm}}} \quad (3)$$

where the heat transfer area (A_o) was calculated from the outer surface of the tubes:

$$A_o = n \cdot (\pi \cdot d_o \cdot L) \quad (4)$$

Using the overall heat transfer coefficient, the solution side heat transfer coefficient (h_s) was calculated using the following expression:

$$h_s = \left(\frac{1}{U} - \frac{d_o \ln(d_o / d_i)}{2\lambda_{\text{Cu}}} - \frac{d_o}{d_i h_c} \right)^{-1} \quad (5)$$

The heat transfer coefficient of the cooling water (h_c) was calculated using the Dittus-Boelter correlation given as:

$$\text{Nu}_c = \frac{h_c d_i}{\lambda_c} = 0.023 \text{Re}_c^{0.8} \text{Pr}_c^{0.4} \quad (6)$$

Where the Reynolds number of the cooling water is:

$$\text{Re}_c = \frac{u_c d_i \rho_c}{\mu_c} \quad (7)$$

The degree of subcooling defines the deviation of the solution conditions from equilibrium. This study considered two definitions for the degree of subcooling: the degree of subcooling at the inlet of the absorber ($\Delta T_{\text{sub, in}}$) and that of the outlet of the absorber ($\Delta T_{\text{sub, out}}$), defined by the following equations:

$$\Delta T_{\text{sub, in}} = T_{\text{in}}^{\text{eq}}(P_{\text{abs}}, X_{\text{s, in}}) - T_{\text{s, in}} \quad (8)$$

$$\Delta T_{\text{sub, out}} = T_{\text{out}}^{\text{eq}}(P_{\text{abs}}, X_{\text{s, out}}) - T_{\text{s, out}} \quad (9)$$

High values of the degree of subcooling at the outlet of the absorber ($\Delta T_{\text{sub, out}}$) indicated that the solution was cooled below its equilibrium temperature and refrigerant absorption did not occur fast enough to eliminate or reduce the degree of subcooling. Moreover, $\Delta T_{\text{sub, in}}$ had a significant influence on the operation of the absorber. Higher values of $\Delta T_{\text{sub, in}}$ indicate that the mass transfer process will start more quickly than in those cases where the solution inlet temperature is closer to equilibrium temperature.

The vapour absorption rate per unit mass transfer area can be expressed as:

$$m_{\text{abs}} = \frac{m_{s,\text{in}} \left(\frac{X_{s,\text{in}}}{X_{s,\text{out}}} - 1 \right)}{A_o} \quad (10)$$

In addition, flow configuration in the falling film is defined by the Reynolds number of the film:

$$\text{Re}_{\text{film}} = \frac{4\Gamma}{\mu} \quad (11)$$

Where Γ is the solution mass flow per twice the length of the absorber tube and μ is the dynamic viscosity of the solution.

The overall mass transfer coefficient is defined by the following expression:

$$k_m = \frac{m_{\text{abs}}}{A_o \Delta X_{\text{lm}}} \quad (12)$$

Where the driving potential for mass transfer ΔX_{lm} , defined as a mean value of the concentration gradient existing along the absorber is given as [22]:

$$\Delta X_{\text{lm}} = \frac{(X_s^{\text{eq}} \rho_s^{\text{eq}} - X_s \rho_s)_{\text{in}} - (X_s^{\text{eq}} \rho_s^{\text{eq}} - X_s \rho_s)_{\text{out}}}{\ln \frac{(X_s^{\text{eq}} \rho_s^{\text{eq}} - X_s \rho_s)_{\text{in}}}{(X_s^{\text{eq}} \rho_s^{\text{eq}} - X_s \rho_s)_{\text{out}}}} \quad (13)$$

Where $X_{s,\text{in}}$ and $X_{s,\text{out}}$, are the concentrations of the solution at the inlet and the outlet of the absorber, respectively, $\rho_{s,\text{in}}$, $\rho_{s,\text{out}}$ are the densities of the solution at the inlet and the outlet of the absorber respectively, $X_s^{\text{eq}}_{\text{in}}$ and $X_s^{\text{eq}}_{\text{out}}$ are the equilibrium concentrations defined at absorber pressure and at the inlet and outlet temperatures respectively determined using the correlation reported by Alvarez et al. [15] and $\rho^{\text{eq}}_{\text{in}}$ and $\rho^{\text{eq}}_{\text{out}}$ are the equilibrium solution densities defined at the equilibrium concentrations and the inlet and outlet temperatures of the solution, using the correlation reported by Alvarez [8].

3.5. Uncertainty analysis

An uncertainty analysis of the absorber efficiency parameters was carried out by Álvarez [8]. The efficiency parameters of the absorber were estimated based on direct variables such as measured temperatures, pressures and mass (or volumetric) flow rates, and indirect variables such as the solution concentration in salt at the entrance and exit of the absorber. The solution salt concentration was an indirect measurement that was obtained from the temperature and density of the solution, hence, the uncertainty in estimating the solution concentration also affects the efficiency parameters of the absorber. The propagation law of uncertainty was applied to estimate the uncertainty of each of the efficiency parameters of the absorber [8]. Therefore, the typical uncertainty corresponding to each variable was calculated based on the standard deviation and the accuracy of the measuring equipment. The resulting value was multiplied by a coverage factor (k), corresponding to the desired safety margin, to obtain the limits of the uncertainty interval of the measurement. In the present work, a safety margin of 95% was selected ($k = 2$). The uncertainties of the absorber efficiency parameters are summarized in Table 2.

4. Experimental results and discussion

Experimental tests were performed for a base concentration of 82% by weight of the nitrates solution and an operating pressure of 30.0 kPa in the absorber. The flow and temperature of the cooling water, and the solution flow rate at the entrance of the absorber were varied to evaluate the effects on each of the efficiency parameters of the absorber. The effect of pressure and concentration of the solution at the inlet of the absorber were also investigated. The operating parameters of the absorber were evaluated at a pressure of 35.0 kPa and were compared with the results obtained for 30.0 kPa. Similarly, the operating parameters of the absorber were evaluated at a concentration of 75% by weight of the nitrate solution and compared with the results obtained under the conditions of the base case (82% by weight).

4. 1. Sensitivity study

A sensitivity analysis of the operating parameters of the absorber was performed for different input variables.

4.1.1. Effect of cooling water flow rate and temperature

Typically, high flow rates of cooling water are used in horizontal tube falling film absorbers to ensure a fully turbulent flow and high heat transfer coefficients. This guarantees that the absorption process is not limited by the cooling water side. Miller [23] suggested operating at Reynolds numbers above 42000. In this study, it was not possible to achieve Reynolds values that high, however, tests were carried out varying the flow rate of the cooling water to determine its effect on the performance parameters of the absorber. The flow rate of the cooling water was varied in the range of 150 l.h⁻¹ to 235 l.h⁻¹, corresponding to the Reynolds number between 11330 and 17670. The effect of the cooling water flow rate was investigated at a water temperature of 85 °C. At other three cooling water inlet temperatures (82, 83 and 84 °C), the performance of the absorber was studied at only three different flow rates of cooling water, namely 150, 180 and 200 l.h⁻¹. The objective was to analyse the effect of a cooling water flow at different inlet water temperatures.

The results obtained at an input solution concentration of 82% by weight suggested that the performance of the absorber underwent a continuous improvement with the increase in the Reynolds number of cooling water. Figure 7 shows the effect of the cooling water flow rate on the vapour absorption rate. Increasing the cooling water flow increased the water capacity to remove heat from the absorber, and consequently increased the mass transfer in the falling film. The vapour absorption rate increased from 3.67 to 4.43 g.m⁻².s⁻¹ when the Reynolds number of the cooling water was increased from 11,360 to 17,670 at a cooling water inlet temperature of 85 °C.

Increasing the temperature of the cooling water produced a decrease in the vapour absorption rate (Figure 7). The absorption rate decreased by 19% when the cooling water temperature was increased from 82 to 85 °C. Similar trends were obtained in other studies [23, 24]. The increase in temperature of the cooling water implied a smaller temperature difference between the cooling water and the concentrated solution. This difference

reduced the partial pressure of the solution at the liquid-vapour interface. Reduction of the driving potential reduced vapour absorption rate.

Figure 8 shows the behaviour of the degree of subcooling of the solution at the outlet of the absorber as a function of the Reynolds number of the cooling water. The degree of subcooling increased slightly in the range of solution flow studied with an increase in cooling water flow rate. For a cooling water inlet temperature of 85 °C, the degree of subcooling of the solution at the outlet of the absorber varied between 12.7 and 13.7 °C when the Reynolds number of the cooling water was increased from 11330 to 17670. This trend was because increasing the Reynolds number of the cooling water (for the same solution flow rate) increased the capacity to withdraw the heat of absorption and the absorber cooled the solution more before it left the absorber. The degree of subcooling of the solution at the outlet of the absorber decreased slightly with an increase in the temperature of the cooling water. The high values of the degree of subcooling of the solution, around 13 °C, indicated that at the bottom the absorber was working as a heat exchanger and was causing a cooling of the solution.

4.1.2. Effect of the solution flow rate

The effect of the solution mass flow rate in the range of 0.011-0.021 kg.m⁻¹.s⁻¹, was investigated corresponding to a Reynolds number (Re_{film}) between 7.0 and 13.3. The effect of the solution flow rate was studied at a cooling water flow rate of 180 l.h⁻¹ ($Re_c = 13171.53$) and a cooling water inlet temperature of 80 °C. Figure 9 shows that increasing the mass flow rate of the falling film in the range studied enhanced the vapour absorption rate from 3.92 to 4.71 g.m⁻².s⁻¹. The increase in the vapour absorption rate is directly related to the absorber thermal load, which increased in the order of 16% when the solution flow rate in the range studied was increased (Figure 9). As the solution flow increased, the solution falling film became uniform and covered a larger area of the absorber at the same time improving vapour absorption. In addition, as the solution flow rate increased, the mixing of the solution between the tubes was greater.

The effect of the solution flow on the heat transfer coefficient of the falling film at two inlet temperatures of cooling water (80 and 85 °C) is shown in Figure 10. The heat transfer coefficient on the film side increased with the solution flow rate. This increase was more

pronounced at lower flow rates, because at lower flowrates there was less wetting of the tubes and consequently a lower heat transfer area. At higher flow rates, above $0.018 \text{ kg}\cdot\text{m}^{-1}\cdot\text{s}^{-1}$ the heat transfer coefficient appeared to have an asymptotic tendency, similar to that of results obtained with water/LiBr [14, 22, 25].

Figure 11 shows the mass transfer coefficient as a function of the solution flow rate at two inlet temperatures of the cooling water, namely 80 and 85 °C. The mass transfer coefficient increased with the solution flow rate in the order of 20%. At a cooling water inlet temperature of 80 °C, mass transfer coefficient increased from 3.6×10^{-5} to $4.5 \times 10^{-5} \text{ m}\cdot\text{s}^{-1}$ by increasing the solution flow rate from 0.010 to $0.021 \text{ kg}\cdot\text{m}^{-1}\cdot\text{s}^{-1}$ whereas at 85 °C the increase was 3.3×10^{-5} to $4.0 \times 10^{-5} \text{ m}\cdot\text{s}^{-1}$ brought about by varying the solution flow rate within the same range. Also, it was evident that the mass transfer coefficient decreased by an average value of 12% when the cooling water temperature was increased from 80 to 85 °C, due to the reduction of the mass transfer gradient at the liquid-vapour interface.

It is important to note that the solution distributor allowed a uniform flow to be maintained through the tube bundle in the flow range studied. The results shown were based on the consideration that the tubes were completely and uniformly wet. However, although acceptable wetting of tubes was observed, at low flow rates tube wetting was not complete. When the solution flow rate increased, a better wetting of the surface was observed.

A photographic record of each experimental test, made it possible to show the effect of the decrease of the wetting area of the tubes when the solution flow rate was reduced. In Figure 12, photographs of the solution falling film on the bundle of horizontal tubes are shown for two different solution flow rates. When the solution flow was increased from $0.010 \text{ kg}\cdot\text{m}^{-1}\cdot\text{s}^{-1}$ ($Re_{\text{film}} = 7.0$) to $0.021 \text{ kg}\cdot\text{m}^{-1}\cdot\text{s}^{-1}$ ($Re_{\text{film}} = 13.2$), a higher wetting of the tubes was observed.

4.1.3. Effect of the absorber pressure

The pressure prevailing in the absorber was controlled through the solution temperature in the generator. The temperature of the solution at the inlet to the absorber was taken from the generator tank and varied depending on the value of the pressure. In order to minimize the effects of subcooling, operating conditions of all experimental tests were adjusted to

obtain a 12 °C degree of subcooling of the solution at the inlet of the absorber for all experiments, and to set the temperature difference between the solution and the cooling water at the inlet of the absorber at 23 °C. These adjustments permit equivalent operating conditions to be obtained for the analysis of absorber performance at two different pressure values.

The driving potential for vapour absorption in the falling film can be expressed as a function of the difference between the partial pressure of water vapour in the vapour phase (operating pressure in the absorber) and the vapour pressure of the solution at the vapour-liquid interface. Increasing the operating pressure of the absorber increased the driving force. Figure 13 shows the effect of the absorber operating pressure on the vapour absorption rate. The vapour absorption rate increased by approximately 15% when the absorber pressure was increased from 30.0 to 35.0 kPa. This significant increase could be explained by the increased potential for mass transfer. In addition, Figure 13 shows the degree of subcooling of the solution at the outlet of the absorber as a function of absorber pressure. This degree of subcooling increased with the increase in the absorber pressure. An increase in the order of 0.7°C was observed when the pressure varied from 30.0 to 35.0 kPa.

4.1.4. Effect of the solution concentration

The effect of the solution concentration on absorber operating parameters was carried out by varying the input concentration of the solution from 82% to 75% (Figure 14). By decreasing the concentration of the nitrate solution, the vapour pressure of the solution increased at the vapour-liquid interface and, consequently, the driving force for the mass transfer decreased. Therefore, a solution with a higher concentration in salts has a greater capacity to absorb vapour until the partial pressure of the water and the vapour pressure of the solution tend to equalize. The vapour absorption rate increased by 10% when the solution concentration was varied from 75 to 82% at the entrance of the absorber. For a solution concentration of 75% in salts, the vapour absorption rate varied between 3.24 and 3.62 g.m⁻².s⁻¹ when the solution flow rate was increased from 0.011 to 0.021 kg.m⁻¹.s⁻¹ whereas for the solution concentration of 82%, the range of variation was 3.57 to 3.97 g.m⁻².s⁻¹.

Figure 15 shows the effect of the solution concentration on the degree of subcooling of the solution at the outlet of the absorber on varying the solution flow rate of at the inlet of the absorber. A slight mean increase of 1 °C was observed in the degree of subcooling of the solution when the solution concentration was varied from 75 to 82% at the entrance of the absorber. This tendency indicated that for higher solution concentrations, heat and mass transfer potentials were greater and therefore the absorption process was more effective and consequently a smaller absorber area was required.

4.2. Comparison with experimental data from literature

Most of experimental studies reported on horizontal tube falling film absorbers in open literature were focused on investigating heat and mass transfer processes with the conventional working fluid mixture water/LiBr. There is scarce information in the literature on the absorption process using aqueous solutions of nitrates as a working pair in absorption cooling cycles. Some data on heat and mass transfer characteristics of the alkylate were obtained by Erickson and Howe [4] for a tubular falling film absorber given in Table 3. Because of the significant differences in the design and operating conditions of the absorber, it would not be appropriate to make a comparison between Howe and Erickson data [4] and the data obtained from this study.

Although no data were available to validate the results obtained in the present work, a comparison was performed with the results obtained from horizontal tube falling film absorbers using water/LiBr as a working fluid mixture and with designs similar to that of the absorber used in the present study. In Table 4, the absorber geometry and operating conditions used in previous studies [14, 23] are presented together with a comparison made for each one of the listed studies. Both Miller [23] and Kyung and Herold [14] performed their experiments using a horizontal tube falling film absorber along the outer surface of the tube and cooling water flowing inside the tube. The first study [23] used an absorber of 6 tubes and in the second study [14] tests were carried out with 4 and 8 tubes.

The values obtained in these studies, including the present work, for the heat transfer coefficients on the film side are different due to variations in the experimental operating conditions. These include the inlet temperature and concentration of the solution, the inlet temperature of the cooling water and the operating pressure in the absorber. However, in

spite of the differences found in the characteristics of these studies, the values obtained in the present work for the falling film heat transfer coefficient are in the same range as those reported by Miller [23] although a significant deviation was observed with the values obtained by Kyung and Herold [14]. As regards the vapour absorption rate, the values obtained in the present study are higher than those obtained by Miller [23] for smooth tubes without additives, and are in the same range as those obtained using additives to improve mass transfer in water/LiBr solution.

5. Conclusions

An experimental setup was designed and built to study the absorption process of aqueous solutions of nitrates (Li, K, Na) in a horizontal tube falling film absorber at the operating conditions of a triple-effect absorption cooling cycle driven by high temperature heat sources. A sensitivity study of the operating variables of the absorber was then carried out to evaluate a series of efficiency parameters for the absorber, such as the absorption rate, thermal load, concentration difference between inlet and outlet, degree of subcooling of the solution leaving the absorber and the falling film heat and mass transfer coefficients.

The tests carried out in the experimental setup confirmed the stability of the working fluid at high temperatures, a low corrosiveness and a wide potential for absorption. The results showed that the heat and mass transfer coefficients and absorption rate decreased with the cooling water temperature and increased with the cooling water and solution flow rates, the absorber pressure and with the salt concentration of the solution entering the absorber. At the operating conditions established in the experimental tests, the absorption rate ranged from 2.83 to 6.55 g.m⁻².s⁻¹, the heat transfer coefficient of the falling film varied between 631.9 and 1715.8 W.m⁻².°C⁻¹, while the mass transfer coefficient was in the range of 2.1-6.0 x 10⁻⁵ m.s⁻¹.

The efficiency parameters of the absorber investigated in the present work had similar values to those reported in the literature for the conventional working fluid water/LiBr with additives used for heat and mass transfer intensification in a similar configuration of the absorber. However, it was not possible to perform a systematic comparison with data from

the literature because the operating conditions of the absorber with aqueous solutions of nitrates are different to those usually employed in conventional horizontal tube falling film absorbers with water/LiBr.

Acknowledgements

This study is part of an R&D project funded by the Spanish Ministry of Science and Innovation (ENE2007-65541/ALT). M. Álvarez acknowledges the receipt of scholarship award (BES-2008-006253) from the Spanish Ministry of Science and Innovation.

References

- [1] Erickson, D. Aqueous absorbent for absorption cycle heat pump. US Patent No. 4 454 724, 1984.
- [2] Erickson, D. High temperature absorbent for water vapor. US Patent No. 4 563 295, 1986.
- [3] Davidson, W.; Erickson, D. 260°C Aqueous absorption working pair under development. Newsletter IEA Heat Pump Center, 4(3), pp. 29-31, 1986.
- [4] Erickson, D.C., Howe L.A. Development of High-Temperature absorption working pair. Winter Annual Meeting of the American Society of Mechanical Engineers, AES 8, pp. 47-53, 1989.
- [5] Erickson, D., Potnis, S., Tang, J. Triple effect absorption cycles. Energy Conversion Engineering Conference, Proceedings of the 31st Intersociety IEEE, pp. 1072-1077, 1996.
- [6] Zhuo, C., Machielsen, C. Performance of high-temperature absorption heat transformers using alkitrates as the working pair. Applied Thermal Engineering, 16(3), pp. 255-262, 1996.
- [7] Álvarez, M.E., Esteve, X., Bourouis, M. Performance analysis of a triple-effect absorption cooling cycle using aqueous (lithium, potassium, sodium) nitrate solution a working pair. Applied Thermal Engineering, 79, pp. 27-36, 2015.
- [8] Álvarez, M.E., Theoretical and experimental study of the aqueous solution of lithium, sodium and potassium nitrates as a working fluid in absorption chillers driven by high temperature heat sources (in Spanish), PhD Thesis, Universitat Rovira i Virgili, Tarragona (Spain), 2013.
- [9] Asfand, F, Stiriba, Y, Bourouis, M. Performance evaluation of membrane-based absorbers employing $H_2O/(LiBr + LiI + LiNO_3 + LiCl)$ and $H_2O/(LiNO_3 + KNO_3 + NaNO_3)$ as working pairs in absorption cooling systems, Energy, 115 (1), pp. 781-790, 2016.
- [10] Park, C.W., Kimb, S.S., Cho, H.C., Kang, Y.T. Experimental correlation of falling film absorption heat transfer on micro-scale hatched tubes. International Journal of Refrigeration, 26 (7), pp. 758-763, 2003.

- [11] Shoji, M., Zhang, X. Study of contact angle hysteresis. *JSME International Journal, Series B*, 37(3), pp. 560-567, 1994.
- [12] Beutler, A., Hoffmann, L., Alefeld, G., Gommed, K., Grossmann, K.y Shavit, A. Experimental investigations of heat and mass transfer in film absorption on horizontal and vertical tubes. *Proceedings of the International Ab-Sorption Heat Pump Conference, Montreal (Canada)*, pp. 409-419, 1996.
- [13] Killion, J., Garimella, S. A review of experimental investigations of absorption of water vapor in liquid films falling over horizontal tubes. *HVAC&R Res*, 9(2), pp. 111-136, 2003.
- [14] Kyung, I-S, Herold, K.E. Performance of horizontal smooth tube absorber with and without 2-Ethyl-Hexanol. *Journal of Heat Transfer*, 124 (1), pp. 177-183, 2002.
- [15] Álvarez, M., Bourouis, M., Esteve, X. Vapor-liquid equilibrium of aqueous alkaline nitrate and nitrite solutions for absorption refrigeration cycles with high-temperature driving heat. *Journal of Chemical and Engineering Data*, 56 (3), pp. 491-496, 2011.
- [16] Laliberté, M. A model for calculating the heat capacity of aqueous solutions, with updated density and viscosity data. *Journal of Chemical and Engineering Data*, 54, pp. 1725-1760, 2009.
- [17] Ally, M. Thermodynamic properties of aqueous ternary solutions relevant to chemical heat pumps. Final Report, ORNL/TM-10258. Oak Ridge National Laboratory, 1987.
- [18] Davidson, W.; Erickson, D. New high temperature absorbent for absorption heat pumps. Oak Ridge National Laboratory. ORNL/Sub/85-22013/1, Energy Concepts Company, Annapolis, Maryland, 1986.
- [19] Aseyev, G. *Electrolytes - Properties of solution methods for calculation of multicomponent systems, and experimental data on thermal conductivity and surface tension*. Begell House Publishers, New York, 1998.
- [20] Nomura, T., Nishimura, N., Wei, S., Yamaguchi, S., Kawakami, R. Heat and mass transfer mechanism in the absorber of water/LiBr convectional absorption refrigerator: Experimental examination by visualized model. *Proceedings of the International Absorption Heat Pump Conference, New Orleans, ASME, USA*, pp. 203-208, 1993.

- [21] Garimella, S. Fundamental understanding of heat and mass transfer in the ammonia-water absorber. Final Report. Prepared for Air-conditioning and Refrigeration Technology Institute, 2007.
- [22] Yoon, J., Kwon, O., Bansal, P., Moon, Ch., Lee, Ho. Heat and mass transfer characteristics of a small helical absorber. *Applied Thermal Engineering*, 26 (2-3), pp. 186-192, 2006.
- [23] Miller, W.A. The Synergism between Heat and mass Transfer Additive and Advanced Surfaces in Aqueous LiBr Horizontal Tube Absorbers. International Sorption Heat Pump Conference Proceedings. Munich, Germany: ORNL/CP -101285, pp. 257-267, 1999.
- [24] Deng, S.M., Ma, W.B. Experimental studies on the characteristics of an absorber using LiBr/H₂O solution as working fluid. *International Journal of Refrigeration*, 22 (4), pp. 293-301, 1999.
- [25] Hoffmann, L., Greiter, I., Wagner, V., Weis, V., Alefeld, G. Experimental investigation of heat transfer in a horizontal tube falling film absorber with aqueous solutions of LiBr with and without surfactants. *International Journal of Refrigeration*, 19 (5), pp. 331-341, 1996.

Figures Caption

Figure 1. Configuration of the triple-effect absorption cooling cycle with a high temperature alkali stage [7]

Figure 2. Dühring diagram (P-T-X) of the triple-effect absorption cooling cycle with a high temperature alkali stage [7]

Figure 3. Schematic diagram of the mini-absorber test stand

Figure 4. Photograph of the internal view of the absorber

Figure 5. External surface area of the absorber tubes

Figure 6. Details of the solution distributor at the top of the absorber

Figure 7. Effect of cooling water flow rate on the vapour absorption rate

Figure 8. Effect of cooling water flow rate on the degree of subcooling of the solution at the absorber outlet

Figure 9. Effect of solution flow rate on the vapour absorption rate and absorber thermal load

Figure 10. Effect of solution flow rate on the falling film heat transfer coefficient

Figure 11. Effect of solution flow rate on the falling film mass transfer coefficient

Figure 12. Photographs of the falling film flowing on the horizontal tubes with a 82% salt concentration, 30.0 kPa of operating pressure in the absorber: (a) solution flow rate of $0.010 \text{ kg}\cdot\text{m}^{-1}\cdot\text{s}^{-1}$ ($Re_{\text{film}} = 7.0$); (b) solution flow rate of $0.021 \text{ kg}\cdot\text{m}^{-1}\cdot\text{s}^{-1}$ ($Re_{\text{film}} = 13.2$).

Figure 13. Effect of operating pressure in the absorber on the vapour absorption rate and degree of subcooling of the solution at the absorber outlet

Figure 14. Effect of solution concentration on the absorption rate

Figure 15. Effect of the solution concentration on the degree of subcooling of the solution at the exit of the absorber

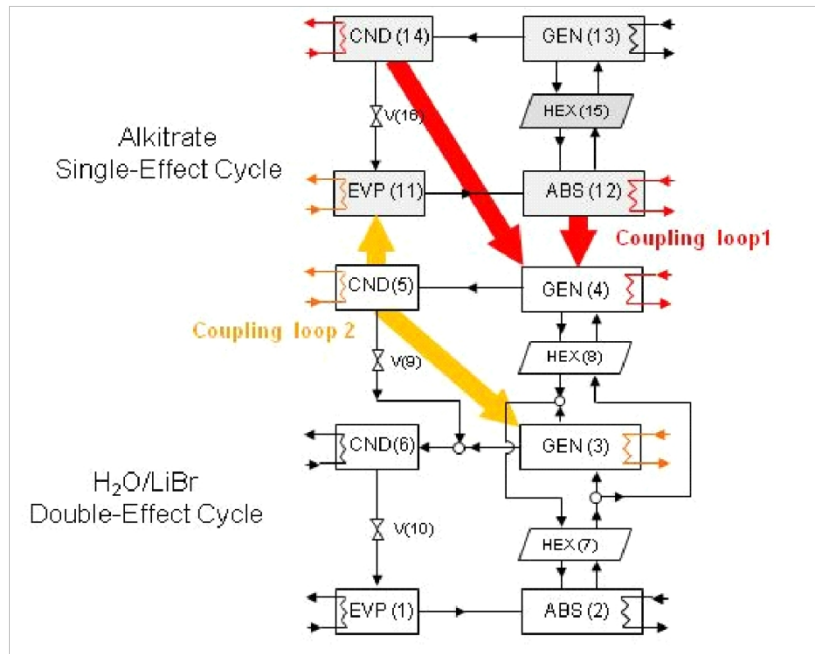


Figure 1. Configuration of the triple-effect absorption cooling cycle with a high temperature alkirate stage [7]

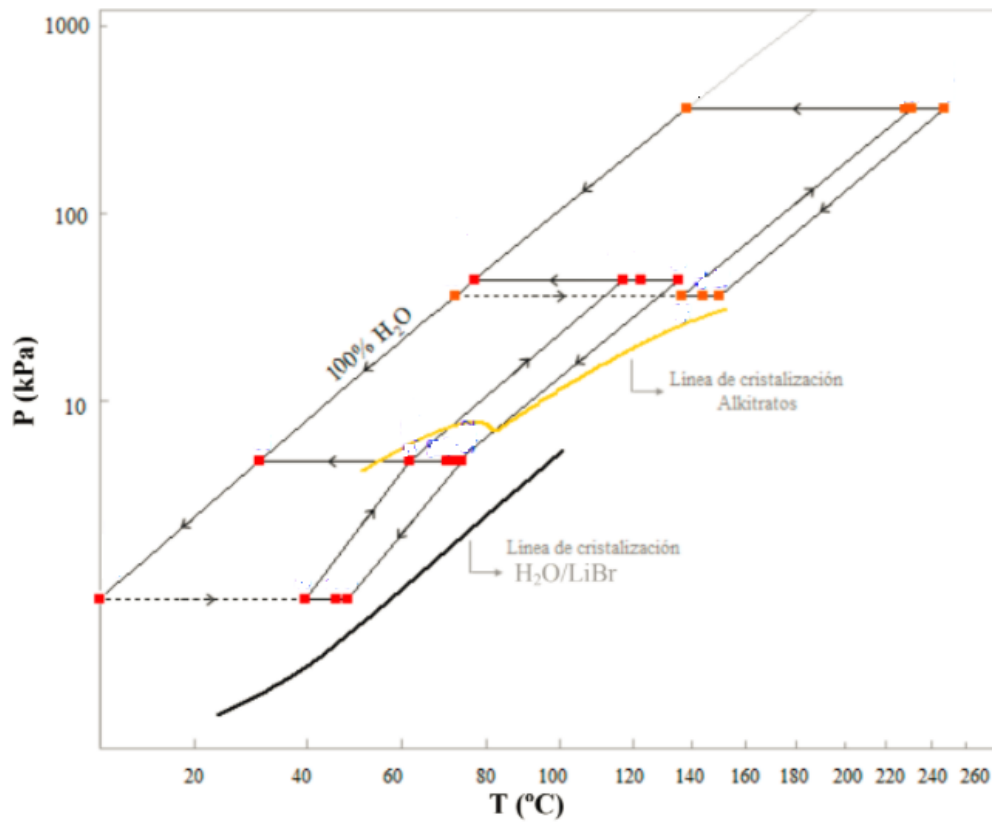


Figure 2. Dühring diagram (P-T-X) of the triple-effect absorption cooling cycle with a high temperature alktrate stage [7]

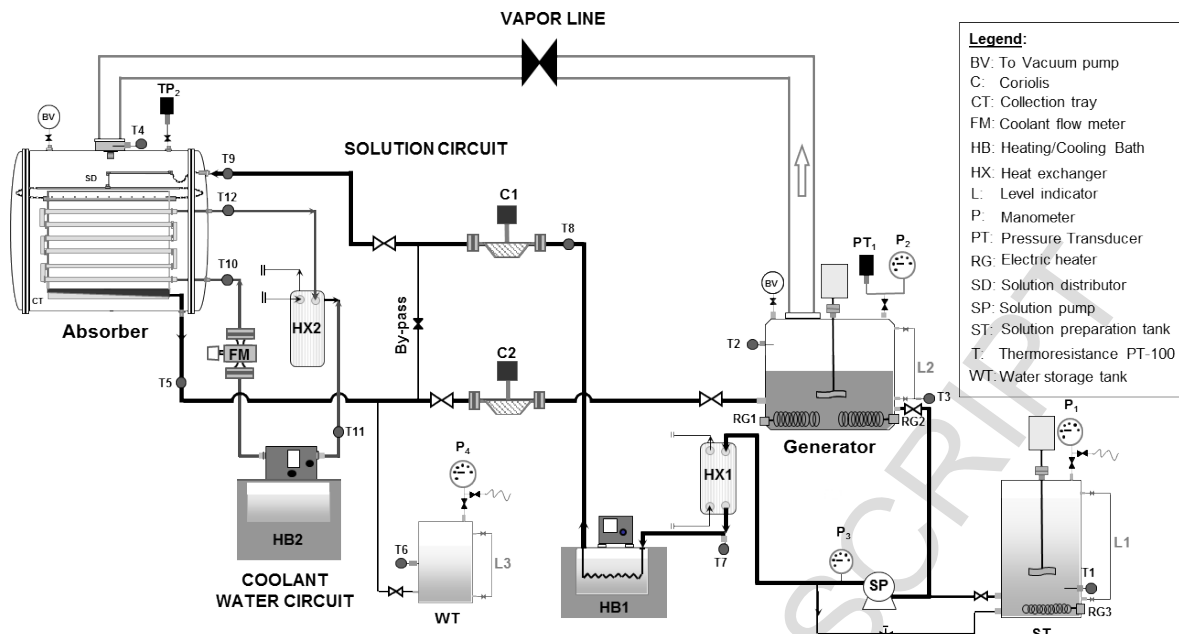


Figure 3. Schematic diagram of the mini-absorber test stand

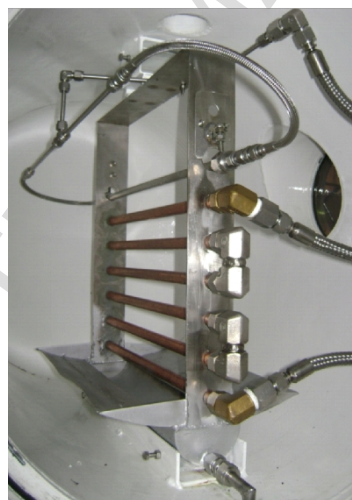


Figure 4. Photograph of the internal view of the absorber



Figure 5. External surface area of the absorber tubes

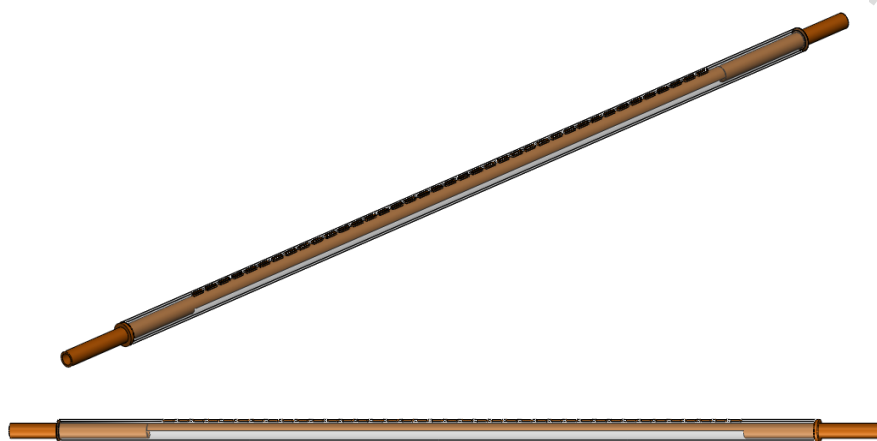


Figure 6. Details of the solution distributor at the top of the absorber

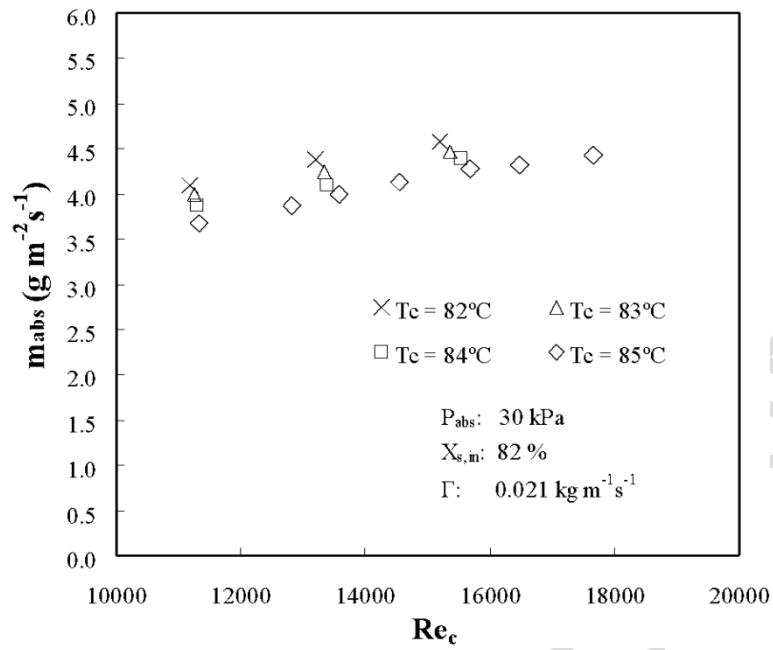


Figure 7. Effect of cooling water flow rate on the vapour absorption rate

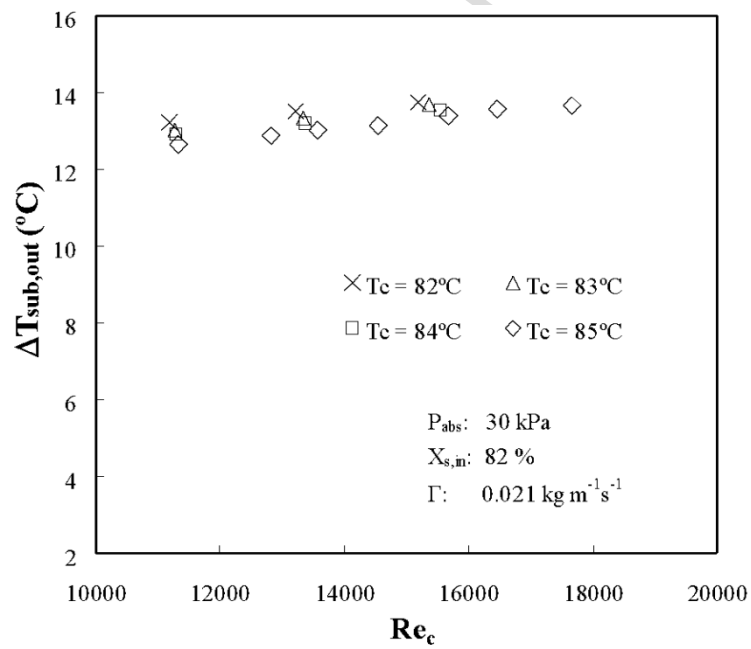


Figure 8. Effect of cooling water flow rate on the degree of subcooling of the solution at the absorber outlet

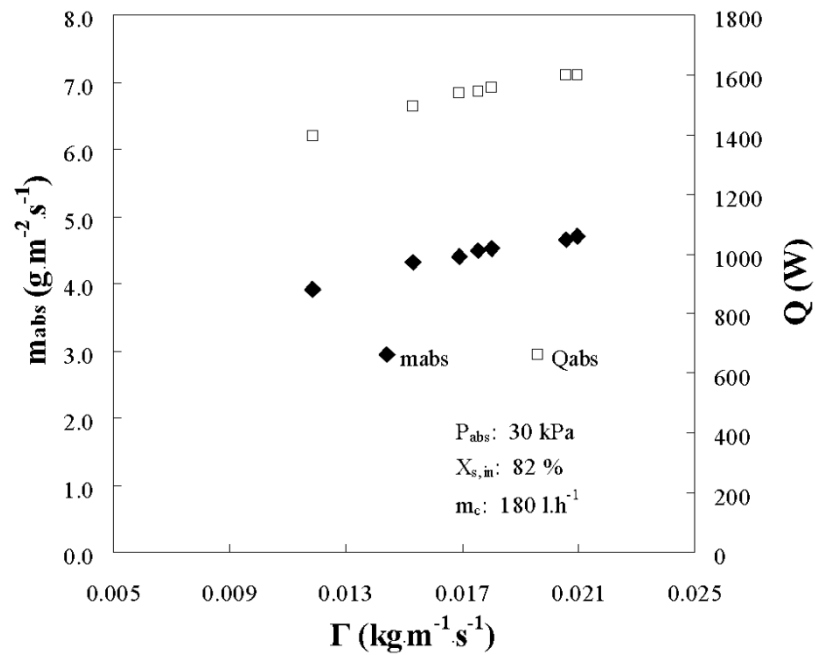


Figure 9. Effect of solution flow rate on the vapour absorption rate and absorber thermal load

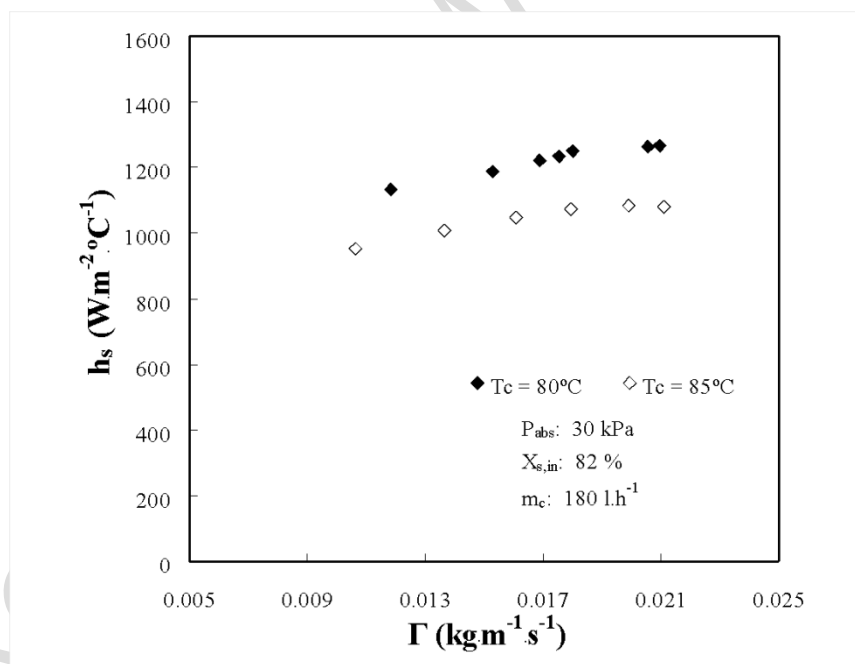


Figure 10. Effect of solution flow rate on the falling film heat transfer coefficient

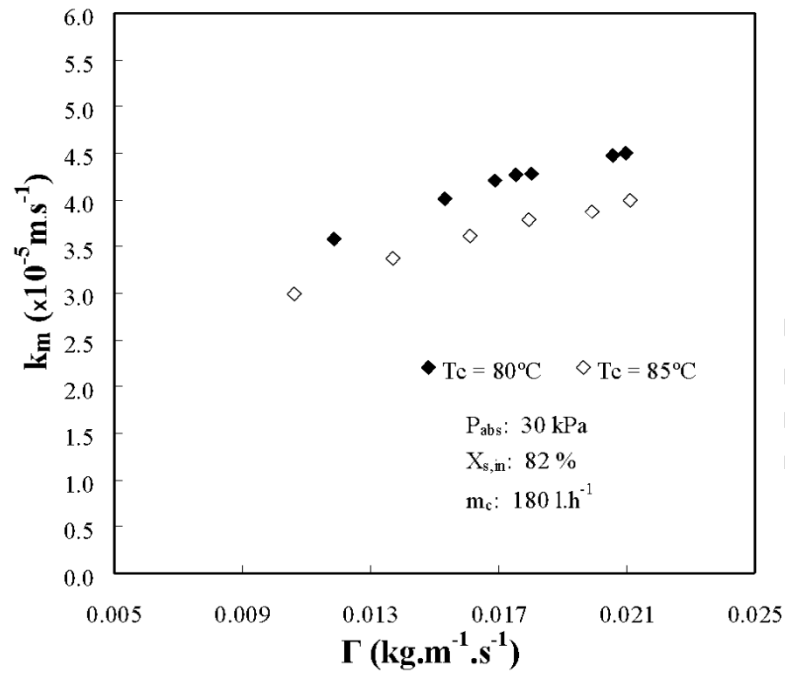


Figure 11. Effect of solution flow rate on the falling film mass transfer coefficient

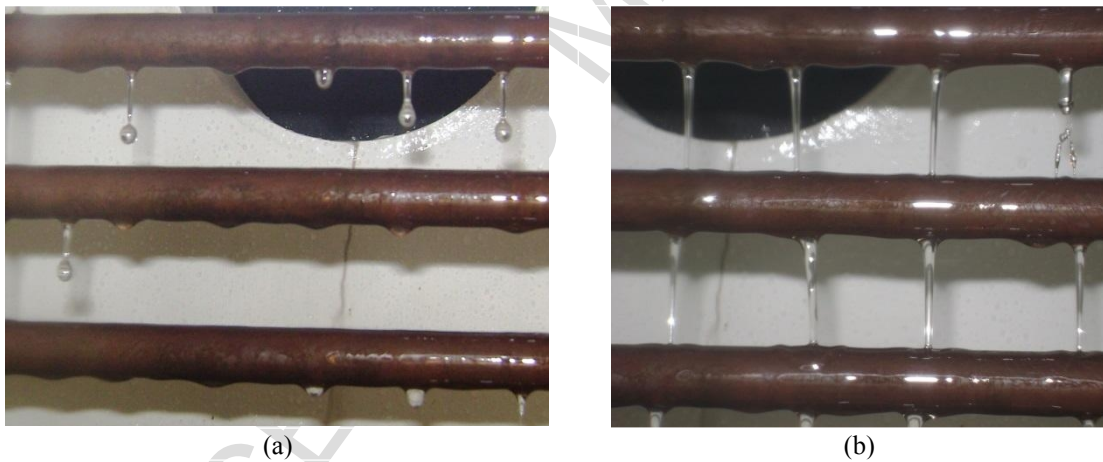


Figure 12. Photographs of the falling film of solution on the horizontal tubes with a 82% salt concentration, 30.0 kPa of operating pressure in the absorber: (a) solution flow rate of 0.010 kg.m⁻¹.s⁻¹ ($Re_{film} = 7.0$); (b) solution flow rate of 0.021 kg.m⁻¹.s⁻¹ ($Re_{film} = 13.2$).

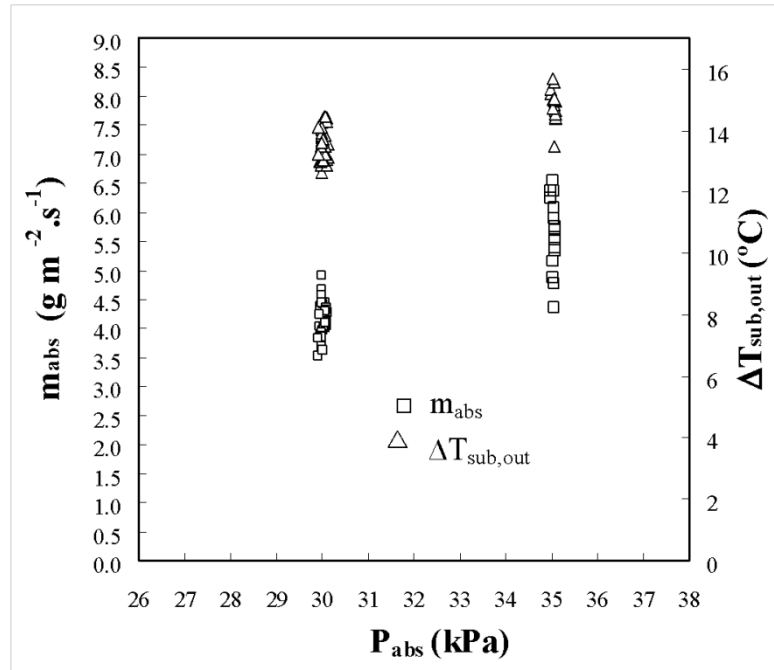


Figure 13. Effect of operating pressure in the absorber on the vapour absorption rate and degree of subcooling of the solution at the absorber outlet

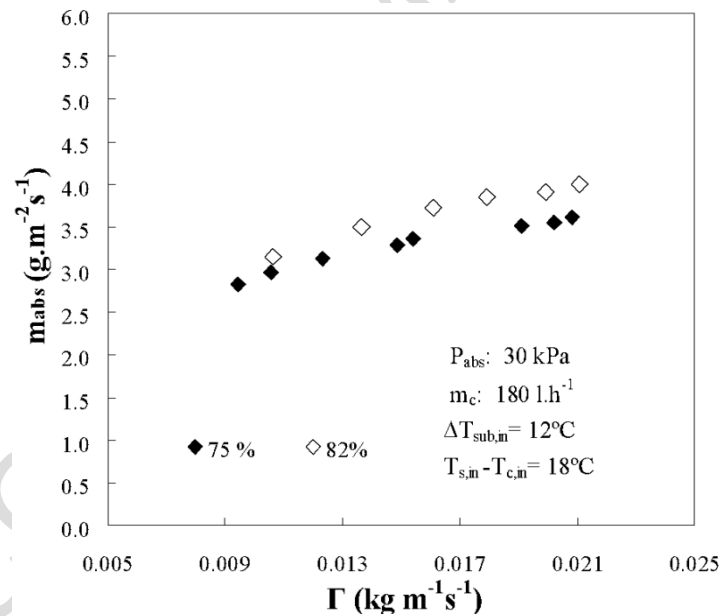


Figure 14. Effect of solution concentration on the absorption rate

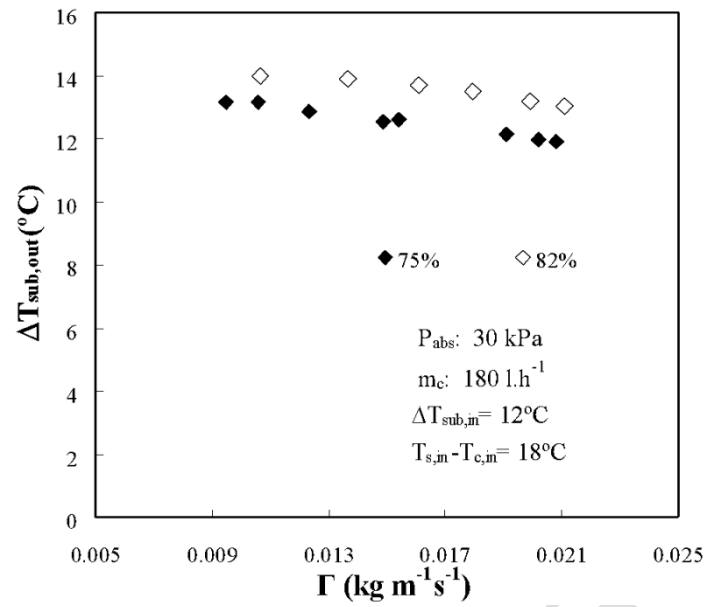


Figure 15. Effect of the solution concentration on the degree of subcooling of the solution at the exit of the absorber

Caption Tables

Table 1. Operating conditions of the experiments

Table 2. Uncertainties of the absorber efficiency parameters.

Table 3. Comparison between experimental data from the literature of falling film absorbers with an aqueous solution of nitrates with those obtained in the present work

Table 4. Comparison of design, operating conditions and performance of horizontal tube water/LiBr falling film absorbers from literature with those of the present work for aqueous solutions of nitrates.

Table 1. Operating conditions of the experiments

Operating conditions	Range of variability
Inlet solution concentration, $X_{s, in}$	82; 75 mass %
Absorber pressure, P_{abs}	30.0; 35.0 kPa
Mass flow rate per unit tube length, Γ	0,010 - 0,021 $\text{kg} \cdot \text{m}^{-1} \cdot \text{s}^{-1}$ ($Re_{film} = 7-26$)
Degree of subcooling of the solution at the entrance, $\Delta T_{sub, in}$	12°C
Cooling water flow, m_c	150- 235 $\text{l} \cdot \text{h}^{-1}$ ($Re_c = 11330-17670$)
Cooling water temperature, $T_{c, in}$	70-85 °C

Table 2. Uncertainties of the absorber efficiency parameters.

Parameter	Average uncertainty (%)
Vapour absorption rate	8
Thermal load	5
Heat transfer coefficient of the falling film	10
Mass transfer coefficient of the falling film	7
Degree of subcooling of the solution at the outlet of the absorber	6

Table 3. Comparison between experimental data from the literature of falling film absorbers with an aqueous solution of nitrates with those obtained in the present work

Erickson and Howe [4]				This study				
Absorbent	Aqueous solution of nitrates (Alktrate)							
Absorber design	Vertical falling film			Horizontal falling film				
Absorber Dimensions	1.52 m length and 0.213 m in diameter			6 tubes of 0.40 m length and 0.016 m in diameter				
Heat transfer area (m ²)	0.1017			0.1206				
Operating Conditions	P (KPa)	X _{s, in} (% in weigh)	Re _{film}	hs (Wm ⁻² °C ⁻¹)	P (kPa)	X _{s, in} (% in weigh)	Re _{film}	hs (Wm ⁻² °C ⁻¹)
	19.0	70	1700	2210	30.0	75	11.9-26.2	632-774
	25.5	70	940	1870	30.0	82	7.0-13.6	951-1318
	26.1	72	130	550	35.0	82	8.4-14.7	1414-1716
	22.7	72	220	700				

Table 4. Comparison of design, operating conditions and performance of horizontal tube water/LiBr falling film absorbers from literature with those of the present work for aqueous solutions of nitrates.

	This study	Miller [23]	Kyung and Herold [14]
Absorbent	Alkitrane	Water/LiBr	Water/LiBr
Number of tubes	6	6	4, 8
Outside Diameter (mm)	16	15.9	19.1
Tube length (mm)	400	320	360, 460
Spacing between tubes	30	12.7, 19.1 and 28.6	24.8
Tube surface	With surface treatment	Smooth and advanced surfaces	Smooth
Operating pressure in the absorber (kPa)	30, 35	0.87	1.23, 1.09
Mass concentration in absorbent (%)	75, 82	60	57, 60
Solution temperature at the inlet (°C)	90-110	NA	37.7 - 52.6
Subcooling of the solution at the inlet (°C)	12	NA	-5.5 - 5.5
Cooling water temperature (°C)	70-90	20-35	30
Cooling water flow (Re_c)	11060-17670	2100-10000	12000
Γ ($kg\ m^{-1}\ .s^{-1}$)	0.010- 0.022	0008-0029	0014-0050
h_s ($W\ m^{-2}\ .^{\circ}C^{-1}$)	632-1716	700-2050	540 0
Absorption rate ($g.m^{-2}.s^{-1}$)	2.83-6.55	(1.5-3.1) no additives; (2.9-6.5) with surfactants and advanced surfaces	NA

NA: Not Available

Experimental characterization of heat and mass transfer in a horizontal tube falling film absorber using aqueous (lithium, potassium, sodium) nitrate solution as a working pair

María E. Álvarez, Mahmoud Bourouis^{1*}

Department of Mechanical Engineering – Universitat Rovira i Virgili,

Av. Països Catalans No. 26, 43007 Tarragona, Spain.

*Corresponding author

Email: mahmoud.bourouis@urv.cat

Highlights

- The absorption process of aqueous solutions of nitrates is investigated.
- The working pair is confined to the last stage of a triple-effect absorption cycle.
- The absorber efficiency is similar to that of water/LiBr with additives.